Team Manitoba
www.iders.ca/auvsi/

AUVSI Student UAV Competition 2005
www.bowheadsupport.com/paxweb/seafarers/default.htm

THE TEAM MANITOBA UNMANNED AERIAL VEHICLE: DESIGN GOALS AND PERFORMANCE

Loren Dueck[♱], Stephen Dueck[1♱], Paul Furgale[♈], Mike Hudek[★], Nike Juzkiw[♱], Jim Majewski[★], Sancho McAnn[♈], Shawn Schärer[♈♱], and Graham Stewart[♱]

[♱] *Department of Electrical and Computer Engineering University of Manitoba*

[♈] *Department of Computer Science, University of Manitoba*

[★] *Department of Mechanical Engineering University of Manitoba*

Team Manitoba has created a camera-equipped unmanned aerial vehicle with a 69 inch wingspan capable of taking off, landing, and navigating between GPS coordinates on its own at a top speed of 65 km/h for 30 minutes (longer if the minimum speed of 33 km/h is used). The search pattern designed by Team Manitoba is useful for airspaces which can accommodate the 800 ft UAV turn diameter. Software for detecting arbitrarily shaped, rotated, and scaled stationary ground targets to enhance human analysis of the video feed, whose integrity is enhanced by a custom-designed antenna, remains under development.

[1] Team Manitoba is attached to the Faculty of Engineering, University of Manitoba, Winnipeg, MB, Canada R3T 5V6. Correspondence may be directed to sdueck@ieee.org.

Loren Dueck is also with Micropilot, Inc. P.O. Box 720, 72067 Road 8E, Sturgeon Rd., Stony Mountain, Manitoba, Canada, R0C 3A0. Stephen Dueck is also with IDers, Inc., 100 - 137 Innovation Drive, Winnipeg, Manitoba, Canada, R3T 6B6. Mike Hudek is also with the Composites Innovation Centre, 301-135 Innovation Drive, Winnipeg, Manitoba, Canada, R3T 6A8. Nike Juzkiw and Jim Majewski are also with Bristol Aerospace, Ltd., 660 Berry Street, P.O. Box 874, Winnipeg, Manitoba, Canada, R3C 2S4.

Created May 18, 2005; Modified June 24, 2005; v.3.1

1. INTRODUCTION

1.1 Motivation

The characteristic benefits of using an aerial platform in warfare include speed, range, lethality, and reduced probability of both detection and interception. A human has historically been required on-board the aircraft to perform somewhat algorithmic tasks such as the maintenance of stable flight and navigation in addition to much more subjective duties such as intelligence gathering and target engagement. Within the last 20 years, however, the following enabling technologies have reduced the need for on-board human decision making:

- over-the-horizon navigation systems such as GPS and communications satellites;
- high-bandwidth communication channels and high-resolution active and passive visioning technology; and
- high instruction and data rate computing platforms coupled with abstract software languages.

Reduced on-board human decision making is advantageous because, in short, the on-board human is a liability to achieving the characteristic benefits within present aircraft designs and a hindrance to achieving performance limits set by structural strength alone. This liability arises due to relatively small tolerable deviations from the temperature, pressure, chemical and force equilibria at which the human body prefers to exist. Furthermore, it is also likely that the quality of the human decision-making process would benefit from being off-board as engagement decisions could be made by a well-rested pilot watching a monitor in a hardened bunker as compared to a flight-weary pilot in the midst of exploding anti-aircraft fire.

Aircraft with off-board human decision-making have historically been referred to as drones or remotely piloted vehicles but presently are called *unmanned aerial vehicles* (UAVs). The change in label reflects the emergence of a new characteristic benefit of aircraft – "persistence" [Gubl05]. This is to say that contemporary aircraft with off-board human decision-making are no longer single-use vehicles as cruise missiles and target drones are.

In general, the present interest in UAVs is due to their potential to complement human decision-making by performing tasks which are dull, dirty, or dangerous. The assumption of these tasks by a UAV reduces an aircraft operator's exposure to risk and allows either present vehicles, unencumbered by a human presence, to operate at higher performance or new smaller vehicles to be employed. These promises aside, however, what is actually required is an engineering development effort. And one which, of course, balances the cost of effort against the benefit expected from the solution of a carefully-chosen problem.

To re-visit the notion of "dull, dirty, and dangerous", a dirty environment is one which is either unpleasant due to a contaminant such as a smoke or one which possesses a non-lethal health threat such as chemicals or radiation. A dangerous task is one in which the loss of human life is certain or where the probability of aircraft/human loss is minimal but the consequences are significant. Examples of the latter include the footage of downed American aircrew shown on Al Jazeera or the media coverage of Capt Scott O'Grady's recovery in June 1996 from the woods of Bosnia after his F-16 was downed.

Lastly, dull problems occur on both large and small scales and include the management of assets which are geographically distributed or which require a persistent high-altitude resource such as a sensor or communications node. Consider, for example, the following observation:

> *The aircraft are armed with air-to-air missiles but basically, we just report any unidentified aircraft, take some pictures and send it all up the NATO command chain.*
>
> - *Sqn Ldr Storr, stationed with NATO forces in Lithuania [RAF05]*

Alternately, dull problems can also include the mitigation of high-impact liabilities such as mobile SCUD missile launchers or ethnic cleansing teams, such as those encountered in Kosovo, [VMPS01] which occur either spuriously or in physically remote locations. Lastly, dull problems can arise at a lower level of automation like the management of large aircraft such as jetliners used in civil aviation. It should be noted that the current trend, in fact, is quite obviously towards reduced human control in the management of large aircraft and it is hoped that UAV research and development will contribute to reducing pilot error as the leading cause of hull loss accidents [2], facts which are exhibited in Fig. 1.1.1 and Fig. 1.1.2.

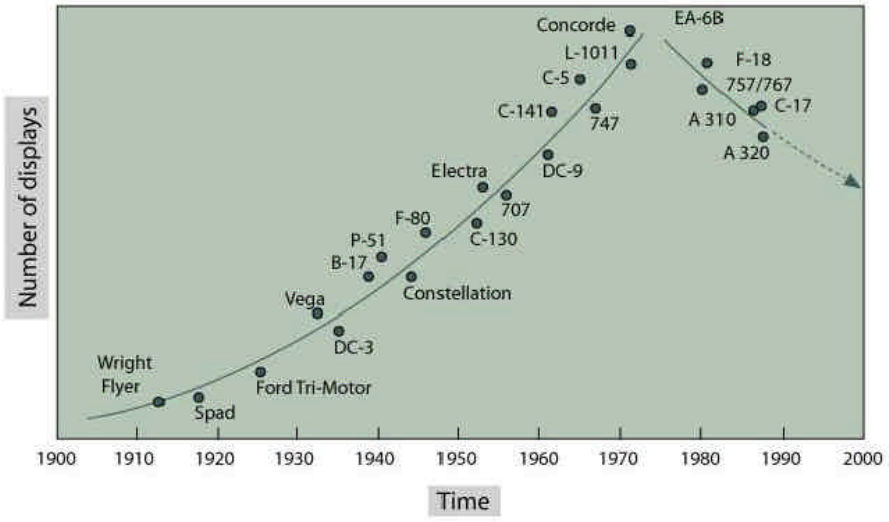

Fig. 1.1.1 Trends in the number of displays in commercial aircraft (from [HaCu04]).

[2] Hull loss is airplane damage that is substantial and is beyond economic repair and includes events in which the airplane is missing or is substantially damaged and inaccessible [Boei04].

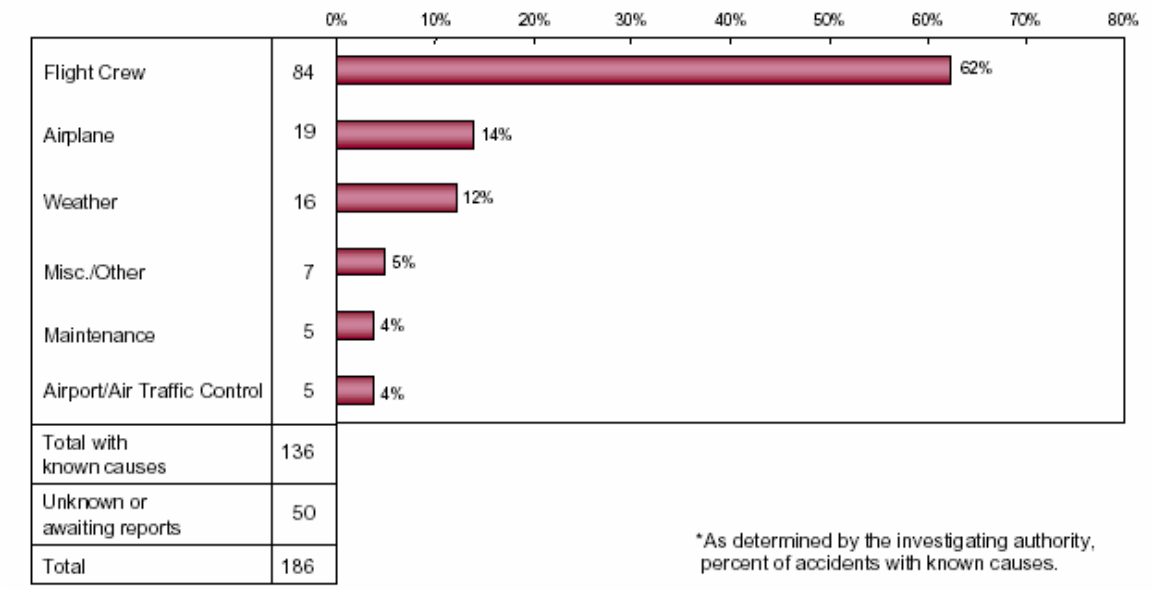

Fig. 1.1.2 Accidents in the worldwide commercial jet fleet resulting in hull loss, 1994-2003 (from [Boei04]).

It is important to note, in the above reference to distributed assets and altitude, that distance is very relative and need not be large. Communication links for mobile, opportunistic combat teams and questions such as "what's over the next hill?", for example, need not be solved or answered by a stealth UAV flying at the edge of space. In short, significant contributions are possible with reasonable effort under the recurring military themes of

- command, control, and communication,
- intelligence, and
- re-supply.

Additional applications for UAVs are shown in Table 1.1.1. Again, it should be noted that ideas such as "border patrol" can scale from a single building in an urban engagement to an entire coastline being monitored by a drug enforcement agency.

Table 1.1.1 Promising areas of application for UAVs [Mars03].

Pipeline surveillance	Severe weather observation
Communications networks	Offshore oil pollution/spills
Power line surveillance	Ice patrols
Crop spraying	Forest fire observation
Mineral exploration	Hydrological surveys
Disaster response	Border patrols
Precision farming	Shoreline erosion monitoring

UAVs are often classified, by NASA and others, according to whether the plane is to loiter and serve as an opportunistic observation/engagement platform or the UAV is purpose-launched to, say, perform a sensory investigation or deliver a payload of supplies. One such classification is shown in Table 1.1.2.

Table 1.1.2 A system of classification of UAVs by capability [TAAC01].

Classification	Altitude [feet]	Endurance
High-altitude, long endurance	> 45,000	> 24 hours
Medium-altitude, long endurance	> 15, 000	> 24 hours
Tactical	< 15,000	< 24 hours
Mini	< 1,500	~ 10 km
Micro	< 500	5-10 km

An excellent starting point in a cost/benefit sense for any UAV application is the µUAV due its relatively low cost in terms of complexity, development time, and material cost. These features make the UAV itself relatively expendable, easy to repair, operate, and transport by a non-specialized team in the field, and conceptually accessible. A reflection on the origins of amateur radio and Linux suggests the potential of the latter advantage.

1.2 Problem

Specifically, the UAV has the opportunity to fulfill the roles inventoried in Fig. 1.2.1, where the demands placed on the UAV and, hence, required capability are determined by the nature of the target.

The challenge is to choose a control problem to systematize and automate which does not attempt to exceed the capabilities of the automation procedure – whether this procedure is a checklist or a probabilistic neural network. As no system is, as yet, fully autonomous, a human operator, on-board or off-board, must remain fully aware of the functional strengths and weaknesses of all automatic systems designed to replace human function. A failure to chose an appropriate problem in this respect will result in automation of sub-optimal phases of a task and/or the need for the human-operator to expend more energy supervising the automation than when the task was manual. This phenomenon has been long been observed in the commercial jetliner industry [Wien89].

Therefore, Team Manitoba restricts its design problem to that of intelligent *intelligence, surveillance, and reconnaissance* (ISR) only – and not the automated delivery of munitions. Furthermore, in the interests of simplicity, targets will be stationary and restricted to a small geographic region, where "small" will be defined as a region easily traversed by a human in a small period of time. This is to say that the ISR tasks will not be time-sensitive as time-sensitive tasks are most likely better left to UAVs in longer endurance classes than µUAVs.

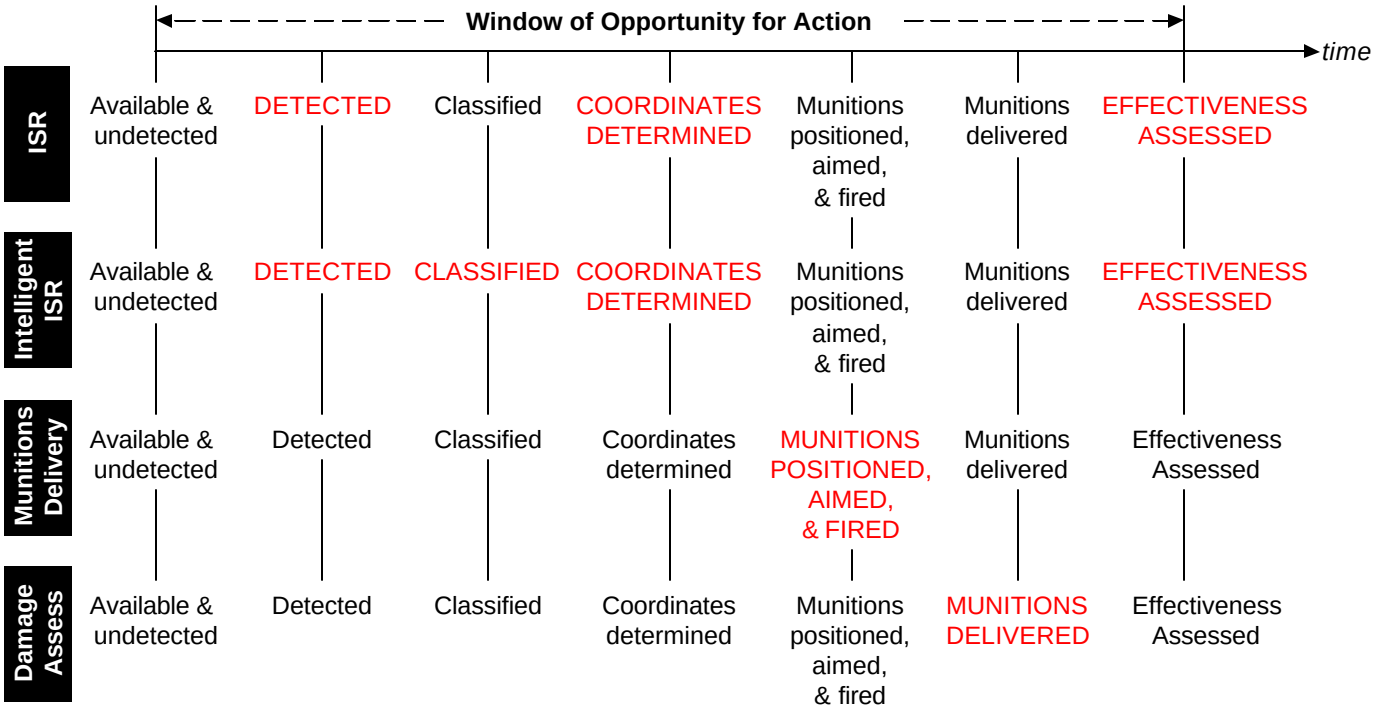

Fig. 1.2.1 Inventory of target time intervals to be minimized for optimal engagement with the UAV potentially performing in different roles.

1.3 Objectives and Document Organization

The aims of this document will be the following:

- to design a µUAV and an experiment to measure its performance (Sec. 2);
- to implement the design in effective manner (Sec. 3 – Sec. 7); and
- to infer its capability from its experimental performance (Sec. 8).

2. SYTEM DESIGN

The essential elements necessary for an µUAV capable of ISR are as follows:

- a stable aerodynamic platform;
- sensors to gather data for stable flight maintenance and guidance;
- an imaging system;
- telemetry and image transmitters/receives;
- an autopilot guidance system; and
- ground control station.

The Team Manitoba design choices in the above areas are summarized in Fig. 2.1 and discussed in greater detail in the below sub-sections. In general, the system was kept as simple as possible so it could be understood to a greater depth and so a balance could be struck between equipment cost and sponsorship successes.

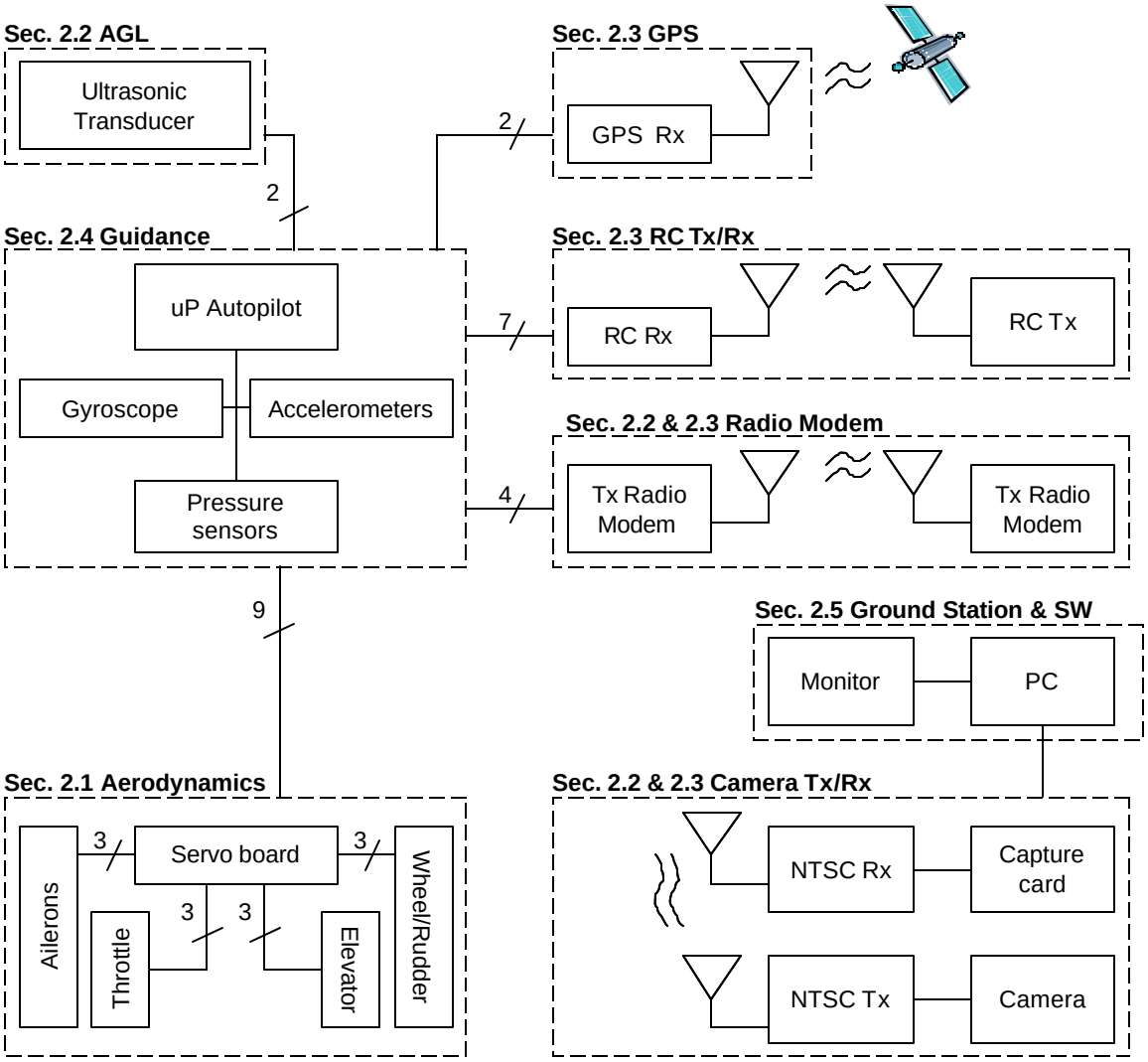

Fig. 2.1 Team Manitoba µUAV system overview.

2.1 Aerodynamic System Design

The aerodynamic system design is a stock, pre-built model aircraft from Hanger 9 called the Extra Easy 2. A stock aircraft was used because this is the first entry by Team Manitoba and the decision to submit an entry was made only 4 months before the competition. Despite the decision to use a stock airframe some slight modifications of the aircraft design were required to accommodate the electronics, camera, an extra fuel tank, flight control sensors and antenna. Effects the modifications would have on airframe structural strength, drag, wing performance and centre of gravity were considered. Several design calculations had to be performed to ensure the aircraft maximum speed and stall speeds would be appropriate for the aircraft mission if the Extra Easy 2 airframe was going to be used in it's stock configuration. In addition the team had to ensure that the aircraft could carry the additional payload required to carry the electronics, antenna, batteries and extra fuel required to complete the mission.

2.1.1 Drag Estimate

The stock aircraft was fitted with a Micropilot autopilot system. The aircraft was test flown and the maximum speed of the aircraft was estimated by averaging the maximum airspeed output by several flight passes. The maximum speed was estimated to be 65 km /hr. In order to calculate drag from the maximum speed the aircraft thrust and lift coefficient of the wing were required.

3.1.1.1 Thrust

The thrust of the 0.46 in^3 Evolution engine and 10 x 6 propeller combination used on the Extra Easy 2 was assumed to be equal to the static thrust of the engine and propeller combination. Typically thrust decreases with forward velocity, however, as a basic estimate of the aircraft drag this assumption will do. One of the team members used to work with the UMSAE Aero Design team. This team measured static thrust of their K&B 0.61 in^3 engine with a 12 x 6 propeller at 31.2 N at 11,000 rpm.

While the Evolution and K&B engines are not the same brand they are of similar engine class. Thus the power of the engines and rpm that they turn a recommended propeller for their size should be similar. Therefore assume that the thrust difference between the two engines will be a ratio of their propeller disc areas. The propeller disk area of the 0.46 engine 10 x 6 propeller combination was 70% of that of the 0.61 engine 12 x 6 propeller combination. Assuming both engine and propeller combinations turned at nearly the same RPM at full throttle it was assumed that the 0.46 engine 10 x 6 propeller combination would move roughly 70% of the air of the 0.61 engine 12 x 6 propeller combination. Thus the static thrust of the 0.46 engine 10 x 6 propeller combination would be roughly 70% of the K&B engine with 12 x 6 propeller, 21.8 N.

3.1.1.2 Wing Lift Coefficient

The wing lift coefficient, C_L, was estimated by comparing a tracing of the wing airfoil to the library of airfoils in the Profili 2.18a software. This library contains over 2200 airfoils. The SPICA airfoil was a very close match to the airfoil used on the Extra Easy 2. Therefore the team estimated the C_L of the wing at stall as the C_L predicted by the Profili software for the Spica airfoil at stall, approximately 11° angle of attack (AOA), C_L = 1.43. Inspection of the Profili 2.18a predicted C_L vs AOA curve and C_D vs AOA curve showed stall began to occur at 11° AOA.

Given the thrust = 21.8 N and the C_L = 1.43 the parasitic drag coefficient of the aircraft was estimated in the following manner.

At maximum speed, 65 km/hr, the total drag on the aircraft equals the total thrust 21.8 N. Drag is a sum of the induced drag, wing profile drag and aircraft parasitic drag defined by equation Eq. 2.1.1. Solving this equation for $C_{D\_para}*A_{Para}$ and inputting know parameters in addition of an assumed e = 0.85 (typical for high wing low speed aircraft) and the AR = 6 and C_{D_wing}= 0.018 (from Profili for the angle of attack required to provide enough lift to support the 4.14 kg aircraft) results in a value for the parasitic drag of the aircraft that is constant with velocity.

$$D = \frac{1}{2} rV^2 * \left(C_{D\_para} * A_{para} + \left[C_{D\_wing} + \frac{C_L^{\ 2}}{peAR} \right] * A_{wing} \right) \quad (2.1.1)$$

$C_{D\_para} * A_{para} = 0.097\ m^2$ or $D_{para} = 19.4$ N.

3.1.2 Estimate Stall Speed of Aircraft when Fully Loaded

The masses of the fully loaded competition ready aircraft and the fully loaded and fueled competition ready aircraft were estimated at 4.34 and 4.95 kg. The stall speed was estimated using Eq. 3.1.2.

$$V_{stall} = \sqrt{\frac{2 * m * g}{C_{L\_Stall} * A_{wing}}} \quad (3.1.2)$$

The stall speed for the unfueled competition aircraft was predicted as 10.8 m/s or 38.9 km/hr. Actual flight testing using the Micropilot controller to provide actual airspeed showed the aircraft actually stalled at about 9.2 m/s or 33.1 km/hr. Thus the team adjusted the C_{L_Stall} value to make the prediction match the real test results and an experimental $C_{L\_Stall\_Exp}$ value was found, $C_{L\ Stall\ Exp} = 1.97$.

The stall speed for the fully fueled competition aircraft was then predicted as V_{stall} fully fueled = 9.8 m/s or 35.4 km/hr.

3.1.3 Estimating Drag at Stall Speed

The drag at the stall speed had to be estimated to ensure the aircraft could lift the full payload. Using equation DDD the drag on the aircraft at stall was estimated using C_L = 1.97 and C_D = 0.025 (from Profili 2.18a predictions for AOA 11°), D = 13.9 N. This is 7.9 N below the estimated maximum thrust of the engine propeller combination on the Extra Easy 2. Therefore, the plane should be able to carry the additional load required to make the Extra Easy 2 mission ready.

2.2 Electronic System Design

The electronics system of the Team Manitoba µUAV consists of 2 distinct but interoperable systems – one for the control of the airplane, and another for imagery to be used in image recognition. In autonomous flight mode, the plane is controlled by an onboard Micropilot 2028g module and accompanying sensors and actuators. Initial flight path programming is done through a 2.4Ghx radio modem operating at 9600baud. This datalink is also used to transmit telemetry data to the ground control station, and to send flight path updates for dynamic re-tasking. The Horizon software package from Micropilot is used to track the plane and issue updates. Ongoing communication with Horizon is not required for successful UAV operation.

The telemetry data transmitted to the ground station is also intercepted by the image processing portion of the ground station to be used in correlating image coordinates with ground position.

The imaging portion of the electronics system consists of a small 8mm CCD video camera and a 900mhz fm transmitter on the plane, transmitting to a ground based receiver.

2.3 RF System Design

The RF system comprises a RC receiver, radio modem, GPS receiver, camera, video transmitter and receiver. All RF system elements are *commercial off the shelf* (COTS) items with the exception of the video receiver antenna (whose construction will be examined in Section 3.3.5). The challenges of using COTS items do not exist in their functional design, but in their overall integration into the aerial vehicle. The lack of a chassis ground on the aerial vehicle (whose construction is entirely balsa wood), complicated by the necessary proximity of the RF elements will inevitably result in RF interference. The sections below will discuss the precautions taken and modifications made to integrate the COTS RF elements into the overall aerial vehicle without compromising their functionality.

2.3.1 RC Receiver

The RC FM receiver operates at 72MHz. The RF stage of the RC receiver demodulates the incoming RC signal (see Fig. 2.3.1 below). If the RC receiver and its lines are unshielded, signals and their subsequent harmonics generated by the radio modem, camera or video transmitter can radiate into the RC receiver's RF stage. This coupling is especially devastating at the mixer of the demodulator, as when the interference is mixed with the local oscillator, new harmonics are produced in addition to the pre-existing fundamentals. As a result, the RC receiver cannot distinguish the transmitted RC signal from all the interference that was radiated into its RF stage.

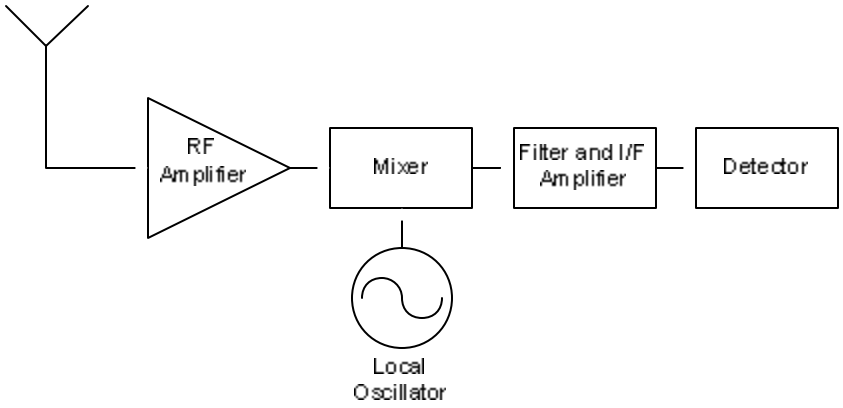

Fig. 2.3.1 RC receiver RF stage (FM demodulation).

Shielding the RC receiver can prevent the problem described above. The RC receiver was wrapped in conductive foil, forming a Faraday cage to protect the receiver from the fields generated by the surrounding RF elements and vice versa. The RC receiver was mounted outside the aerial vehicle to decrease its proximity to the radio modem and video transmitter. The RC antenna (1/4 wave section of transmission line) was mounted horizontally along one aileron wing to isolate it from the video transmitter and radio modem antennas to prevent the antennas from radiating into one another.

2.3.2 Radio Modem

The Microhard radio modem operates at 2.4GHz with a maximum output power of 1W. The radio modem's high output power makes it a potential source of RF interference, especially to the RC and GPS receivers. The radio modem was wrapped in conductive foil that terminated onto its SMA coaxial connector and mounted inside the aerial vehicle body opposite the RC receiver. The shielding will contain any field generated by the radio modem as well as protect the radio modem from any interference generated by other RF elements and electronics (such as the servos). The radio modem antenna (a vertically polarized loaded whip) was mounted on the side of the aerial vehicle body, away from the internal electronics and the RC, video transmitter and GPS antennas.

2.3.3 Video Transmitter and Camera

The Supercircuits video transmitter operates at 900MHz with a maximum output power of 1/2W. The Supercircuits camera is a typical CCT type with NTSC video output. The video transmitter's high power output and the camera's internal oscillator make them possible sources of RF interference, especially to the RC and GPS receivers.

The video transmitter and its antenna were mounted on the aileron wing not populated by the RC antenna. This greatly shortened the length of coaxial cable connecting the video transmitter to its antenna, thus reducing loss and RF leakage. The area of the wing that formed the video transmitter enclosure was nickel sprayed in order to create some from of shielding. The video transmitter antenna is a standard vertically polarized loaded whip. The whip antenna has low gain, but becomes very attractive when its weight, size and durability are considered.

The camera was mounted at the bottom of the plane, below the GPS antenna. It was placed in a plastic enclosure that was wrapped in conductive foil. To prevent the camera's cable from acting as an antenna, it too was shielded. For more detail about the camera's affect on the GPS receiver, refer to Section 2.3.4 below.

2.3.4 GPS Receiver

The GPS receiver operates at 1.57542GHz. The receiver chip is contained in a metal can that is part of the autopilot electronics. The weakness of the GPS receiver lies in its antenna. The GPS antenna is an active antenna with a built in 26dB low noise amplifier (LNA) (San Jose Navigation Inc. PN MK-4). GPS signals are very weak, ranging from –90dB to –150dB prior to amplification. In other words, GPS signals exist well below typical noise floor levels (~-75dB) and therefore can be interrupted by spurious noise, physical obstructions and RF interference. Harmonics generated by the video transmitter

or camera can radiate into the GPS antenna at levels as high as –60dB. Once amplified, these harmonics will be significantly more powerful than the actual GPS signals. Consequently, the noise floor level of the GPS receiver's signal detector will be raised and the actual GPS signals will be interpreted as noise.

The camera was the primary source of interference that impaired the GPS receiver's ability to achieve satellite lock. The interference can be attributed to the camera's internal oscillator and its output cable, whose length is approximately a 1/2 wavelength of the GPS operating frequency, making it a potential antenna. The camera was inserted into a plastic enclosure that was wrapped in conductive metal foil to create a Faraday cage. The camera's output cable was wrapped in foil that terminated on the Faraday cage enclosure and on the output connector. The shielding of the camera and its cable remedied the problem with the GPS not being able to achieve satellite lock. The GPS antenna was mounted on a 4" x 4" ground plane on top of the aerial vehicle body just behind the aileron wing. This is the optimum placement of the antenna as it is not mounted near the engine and has no physical obstructions.

2.3.5 Video Receiver and Antenna

The Supercircuits video receiver operates at 900MHz as a standalone unit. The video receiver is part of the ground station where no strict weight, structural or durability factors are considered. The video receiver comes equipped with a standard vertically polarized loaded whip antenna with approximately 2dBi gain. The whip antenna was replaced with a V-Pole antenna [Lyth05], which is a hybrid of the J-Pole antenna. The V-Pole antenna's gain is approximately 4.5dBi and is extremely simple to construct. The V-Pole was constructed using a continuous piece of galvanized wire. Galvanized wire was selected because its characteristics make the wire act more like a resistor than an inductor, making it easier to tune the antenna to 50 ohms at its coaxial feed point.

The V-Pole dimensions (L1 to L4) are defined as follows (refer to Fig. 2.3.2 below):

- L1: 3/4 wavelength
- L2: 1/4 wavelength
- L3: Coaxial feed-point (the shield is soldered onto L1 and the conductor is soldered onto L2 at dimension L3)
- L4: Element spacing

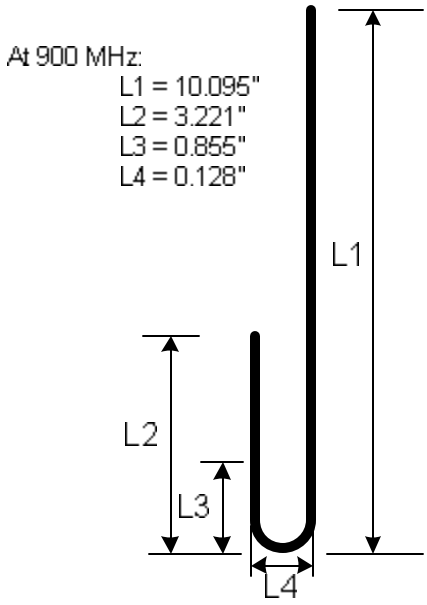

Fig. 2.3.2 V-Pole Antenna

RG142/U was selected as the coaxial cable with BNC crimp connectors. The V-Pole antenna was mounted on a wooden dowel, just below its coaxial feed-point, or alternatively at its lowest Q.

2.4 Guidance

The design of the guidance system was simplified by the use of a Micropilot MP2028 autopilot. For details on the PID loop structure of the MP2028, please read the MP2028 Installation and Operation Manual available at www.micropilot.com.

2.5 Ground Station and Software

The requirements for the target recognition system dictated its design. As the targets will not be announced until the day before the competition, the system must work for arbitrary shapes. It must be able to recognize targets regardless of their size and rotation in the image which will change, depending on the altitude, heading and orientation of the plane. Lastly, the system must be resistant to noise in images.

Program flow for our system is shown in Fig. 2.5.1. Video and telemetry are captured in separate threads. Images are time-stamped, pre-processed and saved to disk and their filenames are pushed onto a queue for pattern recognition. Raw telemetry is parsed and stored in a MySQL database. A pattern recognition thread removes images from the queue and requests interpolated telemetry data based on the image timestamp. This succeeds if there is enough telemetry available for the times surrounding the image. If it succeeds, the image is processed and feature points (points of interest—strong edges) extracted. The feature points are translated into GPS space and sent through a generalized Hough transform that is used to detect arbitrary shapes at any orientation. Targets detected by the Hough Transform are then added to a target pool where they are merged with targets from other images to avoid duplicates.

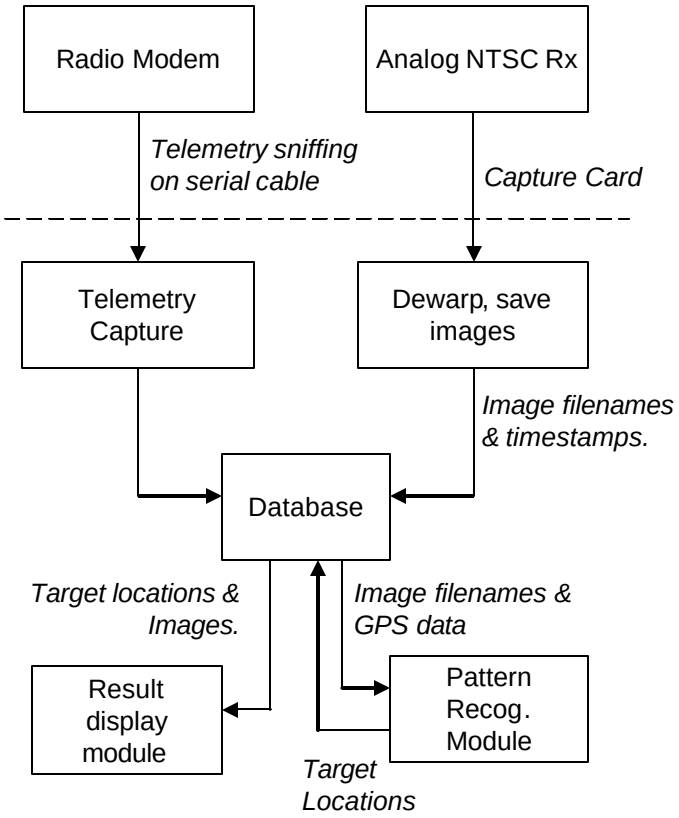

Fig. 2.5.1 Software block diagram and information flow.

2.6 Experimental Design

The objective of the experiment is to evaluate the abilities and difficulties of the Team Manitoba µUAV design in observing stationary targets in a small geographic region.

Specifically, the µUAV will perform the tasks to be performed at the 2005 *Association for Unmanned Vehicle Systems International* (AUVSI) Student UAV competition summarized in Fig. 2.6.1: automated take-off; command-based control; GPS navigation; target search and discovery; and automated landing. The search area is a 500 ft. diameter circle – an area of reasonable usefulness to a mobile combat team performing µUAV surveillance of stationary objects and "small" in the sense that human traveling at, say, 5 km/h could proceed from circle centre to circumference in less than one minute.

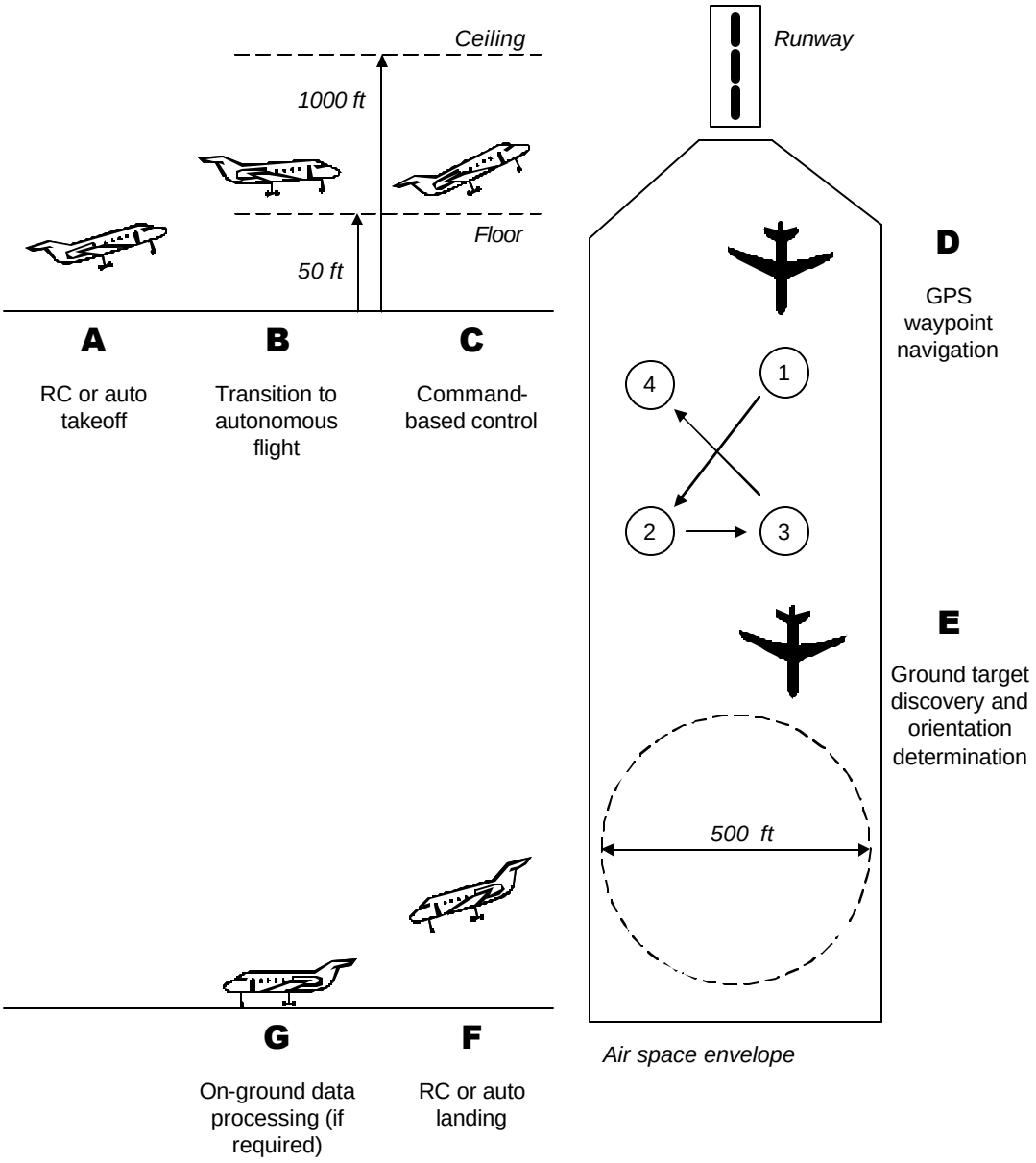

Fig. 2.6.1 Experimental setup.

3. AERODYNAMICAL SYSTEM IMPLEMENTATION

Team Manitoba decided to submit their entry to the AUVSI competition early in 2005. It was decided that since this was the first entry into the competition from this team, a stock airframe should be used to simplify airframe manufacture and design allowing the team to focus on developing the electronic systems of the competition vehicle. The team selected a stable trainer model from Hanger 9, the Extra Easy 2. The analysis described in Sec. 3.1 was performed to ensure that the airframe could support the navigation and surveillance system. Several key areas were investigated through calculations and / or experiment:

- fly slow enough to capture good imagery;
- accommodate the fuel required for the estimated 30 minute competition flight;
- provide enough space for all the guidance and imagery systems; and
- be maneuverable enough to navigate the course.

The following sections provide some details of the Extra Easy 2 vehicle.

3.2 Rudder

The rudder and vertical stabilizer are built from flat plates. The vertical stabilizer has an average chord length of 7 inches with a taper ratio of 0.52. The rudder control surface is an average of 33% of the vertical stabilizer chord. Flight testing showed the aircraft had plenty of yaw control once all the required antennae and other hardware were mounted.

3.3 Wing, H-stab, and Dihedral

The wing has a constant chord of 11.75 inch and a span of 69 inch, resulting in a total wing area of 793 square inches (17.75 square inches are shadowed by the fuselage and are thus not effective lifting surface). The airfoil used in the wing is a flat-bottomed airfoil of shape very similar to the SPICA airfoil found in the airfoil library of Profili Software version 2.18a. The full span ailerons on the wing are 16% of the wing chord length. This is well bellow maximum recommended aileron % of wing chord of 30%. In addition flight testing revealed the aircraft had excellent roll control. The wing incorporates approximately 2° of washout and 3.4° of dihedral. Both of these values are high enough to make the aircraft very stable. The 3.4° dihedral provides a tendency for the aircraft to stay at 0° roll while the 2° washout ensures that the aircraft will not experience tip stalls during the unlikely event of a stall, preventing the aircraft from rolling out of control during stall. The wing also includes Horner style wing tips to reduce wing tip vortices and increase the overall platform efficiency of the wing.

The horizontal stabilizer is a flat plate with a total area of 143 square inches. It is tapered with a straight trailing edge, a taper ratio of 0.7 an average span of 6.4 inch. The elevator has constant chord and is 27.5% of the average horizontal stabilizer chord. This is within the recommended 30% maximum of the average chord before a full flying stabilizer design should be considered.

3.4 Centre of Gravity

The centre of gravity of the aircraft should be located slightly ahead of the centre of lift of the aircraft. Since the horizontal stabilizer on the Extra Easy 2 is a flat plate it was assumed that this surface provided no lift when no elevator input was applied. Therefore it was assumed that the centre of lift of the aircraft corresponds with that of the wing i.e. at the ¼ chord position of the wing or 2.94 inch from the leading edge of the wing. The placement of all the electronics equipment, batteries, extra fuel and antenna was carefully considered to ensure that the centre of gravity remained within 0.5 inches ahead of the centre of lift of the wing. Unfortunately, the team was unable to meet this objective and the final centre of gravity of the fully loaded aircraft and fully loaded and fuel aircraft were 1.19 inches and 0.69 inches aft of the centre of lift of the wing respectively. Due to

the fact that the aircraft was already heavily loaded when fully fueled, the team elected to test fly the aircraft in this configuration. Test flights revealed that the aircraft was indeed stable enough in both the fully fueled and nearly empty configurations. The team may elect to place a weighted spinner on the engine to move the centre of gravity forward if sufficient runway is available at the competition to permit the additional weight to be lifted by the aircraft. This should increase the stability of the aircraft even more.

3.5 Drag and Stall Speed

Team Manitoba selected a pre-fabricated aircraft as their airframe thus the team had little control on the parasitic and induced drag of the airframe. However, efforts were made to minimize the increase in parasitic drag when sensors, electronics and a camera where mounted on the plane.

The team predicted the stall speed for the fully loaded aircraft to ensure that the aircraft would be able to fly slowly enough to allow good maneuverability around the course and good imagery collection. Predicting the stall speed required knowledge of the parasitic and induced drag forces acting on the aircraft. The parasitic drag coefficient was estimated to be 19.4 N at 65 km/hr and the stall speed of the fully loaded and fueled plane was estimated to be 35.4 km/hr using the estimation technique described in section 3.1.

Flight testing of the fully modified aircraft showed that the aircraft began to exhibit stall behavior at 33.1 km/hr. This is within 10% of the predicted value.

3.6 Engine

The 0.46 cubic inch Evolution, Hanger 9 stock engine provided with the Extra Easy 2 airframe was selected for use as it minimized airframe modifications, reduced cost and aerodynamic design changes. Flight testing showed that this engine provided sufficient thrust with a 10 x 6 propeller to get the fully loaded off the ground in approximately 200 feet of runway and very little wind. The static thrust of this engine with a 10 x 6 propeller was estimated to be 4.9 lbf as explained in section 3.1

3.7 Fuel

The stock fuel system of the Extra Easy 2 consisted of an 11 oz fuel tank pressurized by the engine exhaust passing through the muffler. This configuration allowed the aircraft to fly for approximately 12 minutes at near full throttle with a small amount of emergency fuel remaining. Since the competition permits a team 40 minutes to complete the entire mission, Team Manitoba decided to increase the aircraft fuel capacity to allow the aircraft to say aloft for 30 minutes at nearly full throttle. It was anticipated that some time would be required on the ground to process the resulting imagery and that the aircraft would only require 30 minutes to complete the flight portion of the mission. Assuming that endurance would increase linearly with fuel mass (a decent estimate given the fuel would make up approximately 15% of the aircraft mass) the fuel capacity required for 30 minutes of flight was 27 oz.

The fuel capacity of the aircraft was increased to 27 oz by adding a 16 oz tank with its centre of gravity slight ahead of the centre of lift of the wing. This ensured that the

additional fuel did not decrease the aircraft's stability. Unfortunately, to permit easy access to the aircraft electronics, the 16 oz tank which was furthest from the engine had to be mounted 2 inches lower than the 11 oz tank. Ideally the rear tank would have been mounted higher than the forward tank so that the fuel would always flow towards the engine. The fuel system was setup as shown in Fig. 3.1. The carburetor draws fuel from the rear-most, lower 16 oz tank which draws fuel from the forward, higher 11 oz tank. The engine exhaust is used to pressurize the 11 oz tank ensuring that fuel is always flowing to the carburetor. Flight testing showed this system was robust enough and no problems were encountered during the transition from a full to empty 11 oz tank.

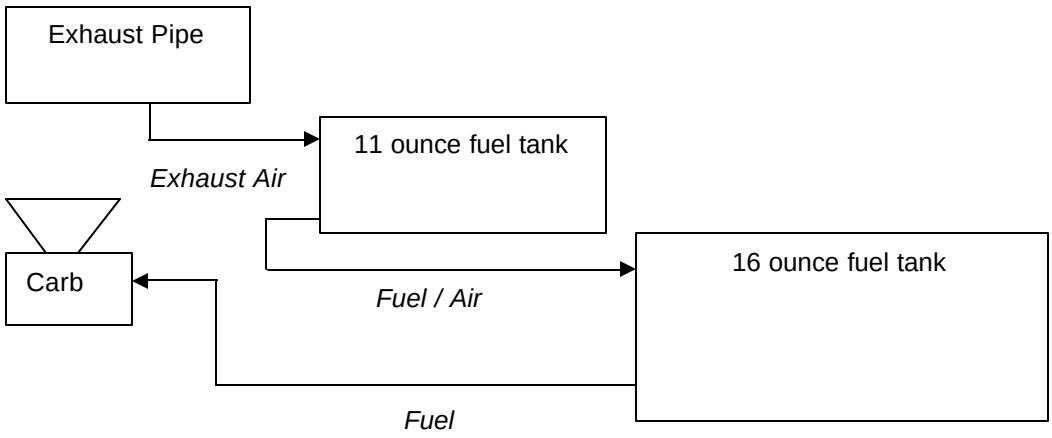

Fig. 3.1 Team Manitoba aircraft fuel system.

During flight testing of the search path the team found that since the aircraft was flying at lower throttle settings to permit more maneuverability and better imagery the aircraft could fly for 25 minutes on as little as 14.5 oz. This suggests that the aircraft could stay aloft for up to 47 minutes.

4. ELECTRONIC SYSTEM IMPLEMENTATION

The system of Sec. 2.2 and Sec. 2.3 are powered by three separate power systems are used within the UAV. The Micropilot and radio modem operate off of a single 6.8V battery. The RC receiver and servo-motors operate off a separate 6.8V battery as the servo-motors require high current in stall conditions and could cause the Micropilot module to reset if the high load voltage of the battery drops below roughly 5V. Both of these batteries are NiCd packs and can be recharged without being removed from the plane. The video camera and transmitter operate on 12-14V and use a separate battery system. A pack made up of 9 AAA format alkaline batteries giving a no-load voltage of 13.5V is used for optimum weight to cost ratio. A custom lithium-ion battery pack was considered; however, in excess of 30 hours of flight with video would be required to justify the cost.

The estimated maximum battery lifetimes from full charge are as follows:

- Micropilot & modem 120mins;
- Servos 90mins; and
- Camera & transmitter 60mins.

5. RF IMPLEMENTATION

For clarity, RF implementation details are discussed alongside their design in Sec. 2.3.

6. GUIDANCE IMPELEMENTATION

Control of the UAV is preformed via the Micropilot MP2028 autopilot. Our implementation (design of the MP2028) relies heavily on the use of GPS for navigation. Using FROMTO GPS waypoints. We can control the plane to move in a straight line from one waypoint to the next. Our implementation utilizes many FROMTO waypoints to form arbitrary flight patterns that the UAV can execute. As tuning the various PID loops of this controller proved both difficult and time consuming various search strategies were employed. They may be viewed in Appendix A.

Given that the complete MP2028 system is a very complex, coupled control system we needed to start at a point that would give us good baseline performance. We decided to use the standard loop parameters that are available in the MP2028 system with the exception of the turn control system. The aileron from roll loop was not modified in our implementation, since by default the aileron from roll loop is already optimized. The heading from crosstrack and the roll from heading loops did not use an Integral parameter by default since this parameter could cause integration windup, but in order to make very tight circle this parameter was needed.

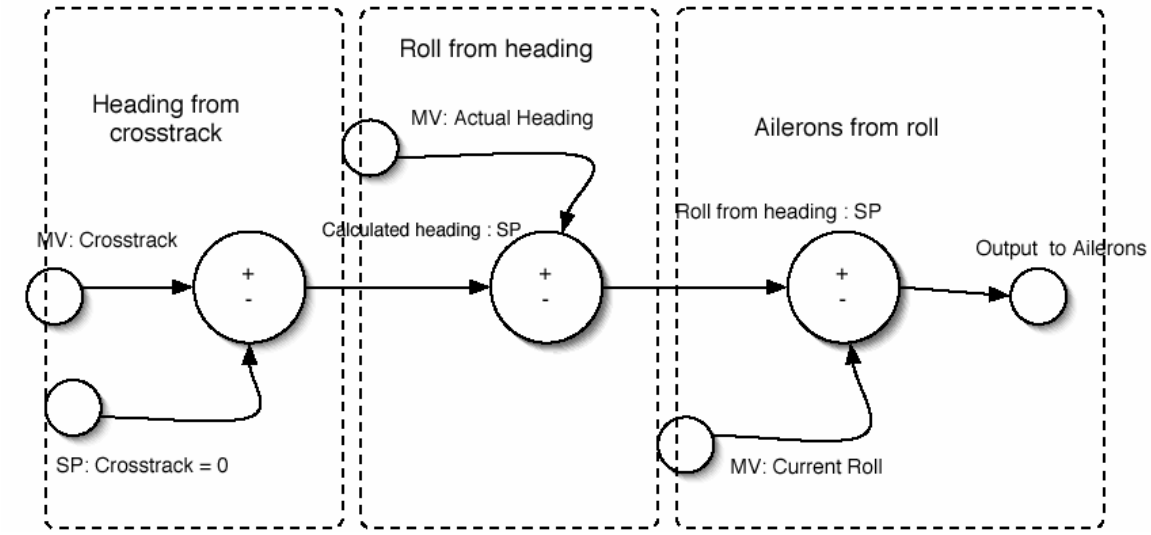

Fig. 6.1 Implementation of turn controller.

Several search patterns were designed based on the search area restrictions of Sec. 2.6 and the airspace restrictions of our airfield. These patterns may be seen in Appendix A. From this it was established the µUAV requires a minimum turn diameter of 483 ft.

7. SOFTWARE SYSMEM IMPLEMENTATION

The software implementation is described below in the context of the block diagram of Fig. 2.5.1 discussed in Sec. 2.5.

7.1 Video Capture

Video is captured using a standard consumer video-capture card using the Video-For-Linux 2 drivers. Images are captured as raw NTSC fields, doubled in height to account for this, and de-warped to account for lens distortion. They are then time-stamped, saved to disk and pushed onto a queue for pattern recognition.

7.2 Image Processing

Our object recognition algorithm requires that we determine areas of interest in the image. We first convert the image to greyscale and apply a median filter to remove high-frequency noise. We use Sobel edge detection to detect strong gradients in the image. By running edge detection vertically and then horizontally, we may determine a local gradient vector for each pixel in the image. The gradient vector represents the first derivative of the luminance at each pixel. These gradient vectors are thresholded by magnitude. The result is a set of feature points (x,y, theta, magnitude) that represent strong edges in the image.

7.3 Pattern Recognition

The pattern recognition block diagram is shown below in Fig. 7.3.1.

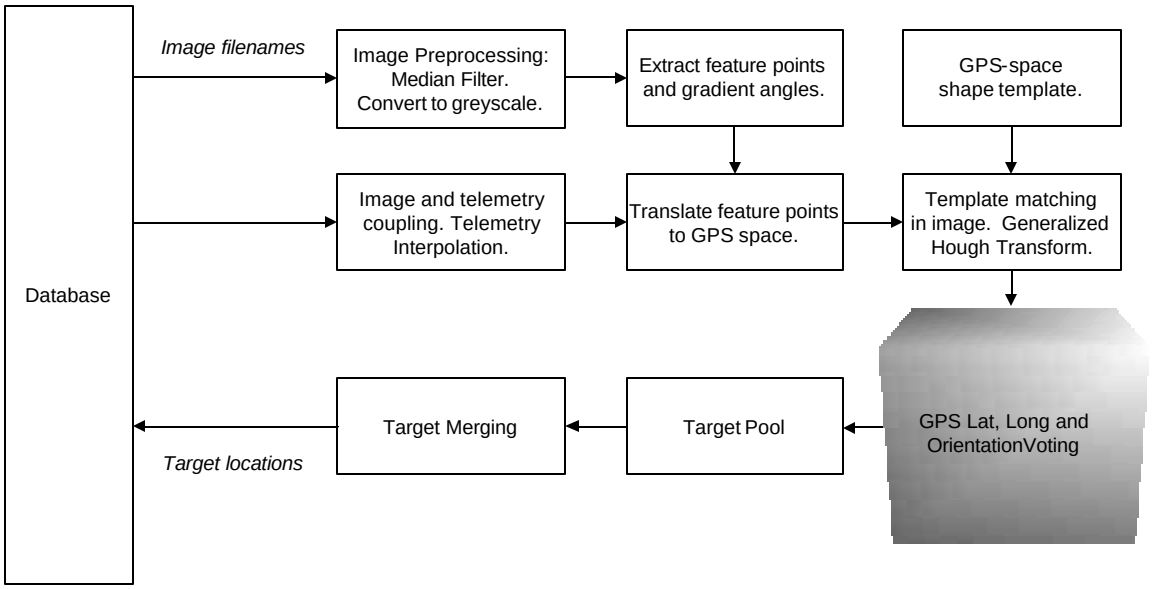

Fig. 7.3.1 Pattern recognition module.

The Generalized Hough Transform is a method used for detecting arbitrary curves in an image using a set of template points to describe the shape of the curve. Template points contain three pieces of information that allow feature points to "vote" for shapes in a voting table called an accumulator. The accumulator is a three dimensional table indexed on x, y of the center point of the shape as well as the orientation of the shape.

To perform the Hough transform, we first specify a template as follows:

- the orientation of the edge at the template point when the shape is at rotation zero;
- the relative orientation of an arbitrary center point; and
- the distance to the center point.

Then, for each feature point $[x_f, y_f, o_f]$ identified in the image

For each point in the template $[o_t, c_t, d_t]$

Determine the implied rotation of the shape.

$$o_{accumulator} = o_f - o_t$$

Determine the implied center point of the shape.

$$x_{accumulator} = x_f + \cos[c_t + o_{accumulator}] * d_t$$

$$y_{accumulator} = x_f + \cos[c_t + o_{accumulator}, * d_t$$

"Vote" at this location.

$$IncrementAccumulator\,[x,y,o]$$

Running this algorithm in image space would require a fourth dimension in the accumulator table for the size of the shape. Rather than account for the size in this way, we transform the image coordinates to GPS coordinates and run the Hough Transform in GPS space. This effectively accounts for differing sizes due to altitude and skew due to perspective distortion.

After processing all feature points, we search the accumulator for local maxima above a certain magnitude. These maxima translate into a GPS latitude, longitude and orientation. Any targets found are added to a list of targets where they are grouped with similar targets from other images for display after the flight.

7.4 Telemetry Capture

Knowing the aircraft's position and orientation is essential for translating a video frame to the world coordinate system. There are two steps in determining the position of the aircraft at a given time. The first is the recording of the telemetry data as it is sent back once per second from the autopilot through the radio modem. The second is using this data to get an interpolated position for the aircraft at the time of each video frame.

With assistance from some documentation from Micropilot, we were able to reverse engineer the protocol used to send the telemetry data. The relevant fields used for positioning the aircraft are the longitude, latitude, altitude, pitch, roll, airspeed, groundspeed, vertical speed, and track fields. As the aircraft's heading was not sent with the data, it had to be estimated using the aircraft's track over the ground, the groundspeed, and an estimate of the winds taken from local aviation surface wind reports and upper air wind forecasts.

Since the video frames are not received at the client in sync with the telemetry data, the telemetry data cannot be used in its raw form to determine the position and orientation data. Some method of interpolation must me used. A linear interpolation between the two nearest data points is not sufficient as it does not take into account the possibility of sensor error, or a non-linear change, which both occur quite frequently in this domain.

The method of locally weighted regression [Mitc97] is the solution we used to allow interpolation, without ignoring sensor error and accounting for non-linear change. It is based on the method of determining a curve of best fit through a set of data points. Finding a curve of dimension n through m points (x,y) can be reduced to the problem of finding the equation:

$$Q(x) = b_0 + b_1 x + b_2 x^2 + \ldots + b_n x^n \tag{7.4.1}$$

which minimizes the sum-squared error:

$$S = [(y_0 - Q(x_0)]^2 + [y_1 - Q(x_1)]^2 + \ldots + [y_m - Q(x_m)]^2 \tag{7.4.2}$$

The solution for $\mathbf{b} = [b_0, b_1, \ldots, b_n]$ that minimizes S is given by the matrix equation:

$$\mathbf{U^T U b} = \mathbf{UY} \tag{7.4.3}$$

where:

$$\mathbf{U} = \begin{bmatrix} 1 & x_0 & x_0^2 & \ldots & x_0^n \\ 1 & x_1 & x_1^2 & \ldots & x_1^n \\ \vdots & \vdots & \vdots & & \vdots \\ 1 & x_m & x_m^2 & \ldots & x_m^n \end{bmatrix} \tag{7.4.4}$$

and $\mathbf{Y}$ is the column vector:

$$\mathbf{Y} = \begin{bmatrix} y_0 \\ y_1 \\ \vdots \\ y_m \end{bmatrix} \tag{7.4.5}$$

To perform this approximation over the entire set of data from the flight would be computationally infeasible, and grossly incorrect using any dimension of polynomial. For this reason, the regression is performed only on a subset of the data close to a requested timestamp. We use boundaries of ±5 seconds to determine this neighborhood.

Here is an example of a best-fit quadratic over a small data set taken from our database (the units for time are in minutes and fractional minutes past midnight, as a decimal format is needed for the multiplication).

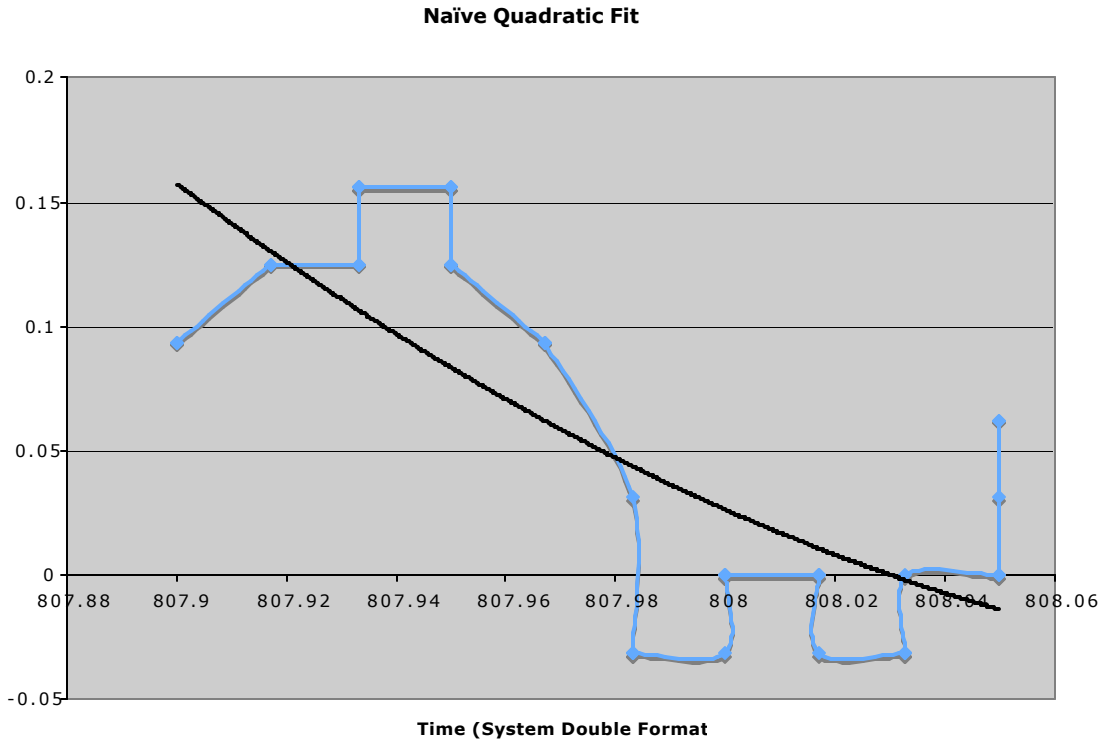

Fig. 7.4.1 Results using a naïve quadratic fit.

A problem with this method is evident in Fig. 7.4.1. Using a low degree polynomial to approximate even a small data set such as this gives a curve that, although it minimizes the sum-squared error over the entire set, is not always as accurate as possible near a given target time. Giving a different weighting to different elements $[y_i - Q(x_i)]^2$ of the sum-squared-error function allows emphasis to be given to points near the target, while still using information from the other points in the neighborhood. The weight to be given to each term is a function of the magnitude $|x_t - x_i|$, where x_t is the target of the interpolation. This function is called the *kernel function* [Mitc97]. Through experimentation, the kernel function we decided on was:

$$k(d) = 1/e^{(100d)^2} \tag{7.4.6}$$

Using the locally weighted regression, the following results are achieved.

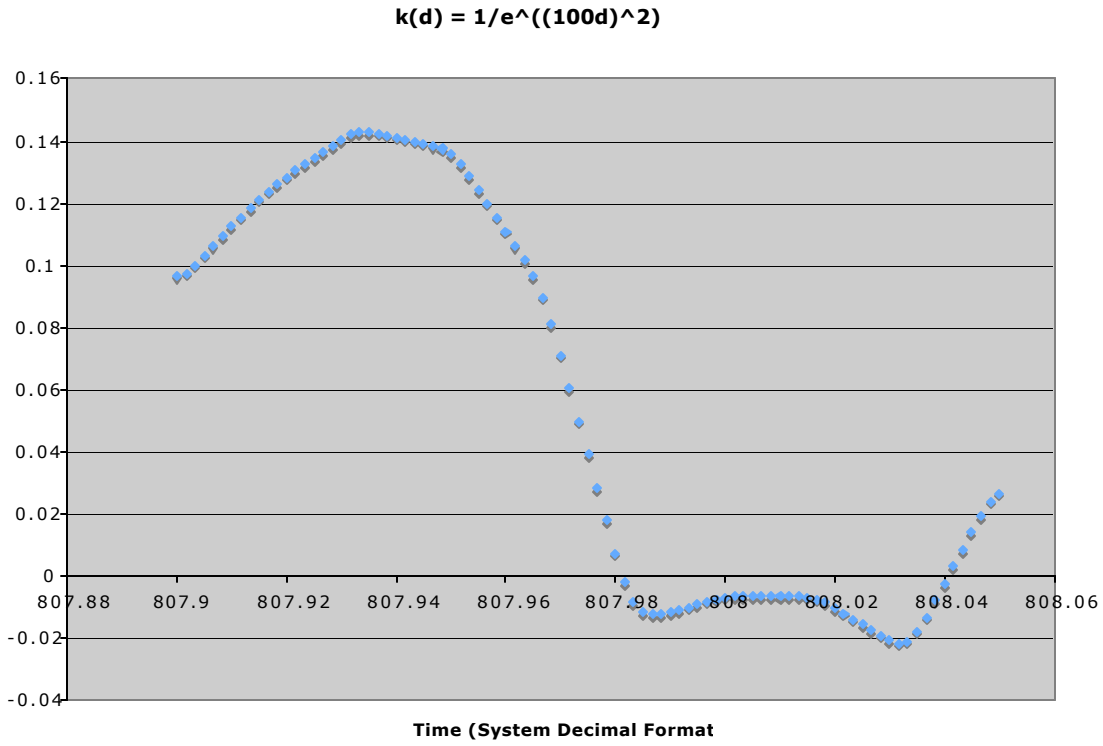

Fig. 7.4.2 Results using locally weighted regression.

This method gives a sufficiently accurate position of the aircraft and is robust to sensor error, transmission dropouts, and non-linear change in any of the values.

8. EXPERIMENTAL RESULTS AND DISCUSSION

The results of Sec. 8.1 were gathered during the approximately 20 flight tests performed by Team Manitoba from February 2005 to June 2005. Their meaning is discussed in Sec. 8.2.

8.1 Results

8.1.1 Automated Take-Off

The µ.UAV is reliably capable of take-off and the acquisition of a set altitude.

8.1.2 Command-Based Control

Testing indicated no problems in the µUAV's ability to dynamically change heading, speed, and altitude using manually-entered software commands.

8.1.3 GPS Waypoint Navigation

The Team Manitoba µUAV is able achieve pre and/or dynamically defined GPS waypoints. However, the waypoints requiring bank must be separated by sufficient

distance so as to allow for a 700 to 800 ft. turn diameter – the smallest we were able to achieve after completing work on more fundamental systems.

8.1.4 Target Search, Locate, and Classification

The inability of our UAV to search the target area within the airspace defined for the experiment is the biggest threat to our success in the experiment. Given a larger airspace, however, a practical search pattern for the 500 ft. diameter circle could be constructed, as shown in Appendix B.

When in a search pattern, the UAV is able to achieve video of sufficient resolution to find a 1x1 m 2D object by flying at 100 ft. The custom designed antenna and cable shielding allowed a video feed relatively free of distortion. Spurious signal integrity issues were present – most significantly due to the corruption of the NTSC signal phase by multi-path effects. The result of phase distortion is an occasional variation in the tint (or hue) of the video.

The classification software is presently able to detect a shape defined via a point-and-click user interface with rotation invariance. Work is still be completed on the image coordinate to GPS coordinate translation. As GPS translation accounts for size differences in images and perspective distortion this improvement would also make the software scale invariant. Consequently, none of the classification section of the system has been tested for generalization in flight.

8.1.5 Automated Landing

The µUAV is capable of landing undamaged on the order of 40% of the time.

8.2 Discussion

The results indicate we have achieved an ISR platform capable of performing surveillance in airspaces which exceed a minimum and reasonably small sized footprint. The system, however, is still missing a fully-understood control system and a target recognition computer incorporating some level of automation. Missile systems such as the highly successful Maverick missile, however, have been in use operationally for years without automated tracking and identification, however, and the "under development" status of our computer does not, therefore, restrict the potential of our aircraft.

9. SUMMARY AND CONCLUSIONS

9.1 Conclusions

This paper began by considering the difficulty and benefits of replacing enough human decision-making on-board an aircraft, creating an *unmanned aerial vehicle* (UAV), to extend human decision-making on the ground. It considered the application of UAVs to the detection of low-probability, high negative-impact events and the potential to achieve this capability at minimum cost through development of a simple, low-maintenance, expendable class of UAVs with limited but non-trivial performance – the µUAV. A µUAV was designed, implemented, and its performance experimentally evaluated by a static target experiment designed and employed by the *Association for*

Unmanned Vehicle Systems International (AUVSI) 2005 Student UAV Competition. The experiment requirement of a 450 ft turn diameter (for the search pattern Team Manitoba has designed) implies Team Manitoba's 700 ft turn diameter is inadequate in the limited context of the experiment. The Team Manitoba µUAV can navigate GPS points and transmit high-integrity video, however – implying a worthwhile intelligence, surveillance, and reconnaissance platform has been created during the 4 months Team Manitoba has been in existence.

9.2 Contributions

In its development effort, Team Manitoba has identified numerous opportunities for collaboration within Winnipeg's significant aerospace and computing sector. It has also integrated a multi-disciplinary engineering effort of high contemporary relevance into the learning environment of the University of Manitoba. Lastly, its members have created a strong technical and organizational foundation upon which future efforts, by themselves and others, can be based.

9.3 Future Work

A critical path goal for improving the Team Manitoba µUAV design include a full understanding of the weaknesses and failure modes of the Micropilot autopilot with a view to creating a custom autopilot. And, in addition, future work will continue development of the of the feature extraction and pattern recognition framework already in place.

10. ACKNOWLEDGEMENTS

Team Manitoba would like to thank Howard Loewen for proposing the formation of a Manitoban AUVSI UAV team and Micropilot for their generous material and financial assistance. Team Manitoba would also like to acknowledge the material support of IDers and the financial support of IDers, the University of Manitoba Faculty of Engineering, the University of Manitoba Department of Electrical and Computer Engineering, the Association of Professional Engineers and Geoscientists of Manitoba, the University of Manitoba Department of Computer Science, and Winnipeg IEEE GOLD.

Thanks are also due to Malcolm Symonds, whose advice helped the team evolve from an interesting idea to an engineering reality, to Pat Fedirchuk for her congenial and capable financial accounting, and John Fleischaker for his excellent graphic design work.

11. REFERENCES

[Boei04] Boeing. *Statistical Summary of Commercial Jet Airplane Accidents Worldwide Operations: Worldwide Operations 1959 – 2003*. [Online] http://www.boeing.com/news/techissues/, 2004. (as of June 22, 2005).

[Gubl05] A. Gubler, "Precision air strike evolution," *Defence Today – Defence Capabilities Magazine*, vol. 4, no. 1, 2005.

[HaCu04] R. J. Hansman and M. Cummings, "Human supervisory control of Automated Systems," Human Supervisory Control of Automated Systems Lecture Notes, 2004. [Online]. http://ocw.mit.edu/OcwWeb/Aeronautics-and-Astronautics/16-422Spring2004/LectureNotes/index.htm (as of June 22, 2005).

[Lyth05] H. Lythall. *VPOLE ANTENNA*. [Online] http://web.telia.com/%7Eu85920178/anrennas/vpole0.htm (as of May 22, 2005).

[Mars03] G. F. Marsters, "Ummmm… So where does the pilot sit?," *50th Annual General Meeting of the Canadian Aeronautics and Space Institute*, April 28, 2003.

[Mitc97] T. Mitchell. *Machine Learning*. McGraw-Hill, 1997, pp. 236-238.

[TAAC01] New Mexico State University Unmanned Aerial Vehicle Technical Analysis and Applications Center (TAAC). *High-Altitude Long Endurance Unmanned Aerial Vehicles Certification and Regulatory Roadmap*. 2001 [Online]. http://www.psl.nmsu.edu/uav/roadmap/ (as of June 23, 2005).

[RAF05] Royal Air Force, "Baltic exchange," *RAF – The Official Magazine*, vol. 1, no. 4, pp. 14-16, 2005.

[VMPS01] A. Vick, R. M. Moore, B. R. Pirnie, and J. Stillion. *Aerospace Operations Against Elusive Ground Targets*. Rand Corporation, 2001. [Online]. http://www.rand.org/publications/MR/MR1398/ (as of June 22, 2005).

APPENDIX A: IDEAL FLIGHT PATH DESIGN

All cases assume minimum height ever flown in 100 ft and camera has a 45 degree field of view and is mounted so it points directly at the ground during a bank.

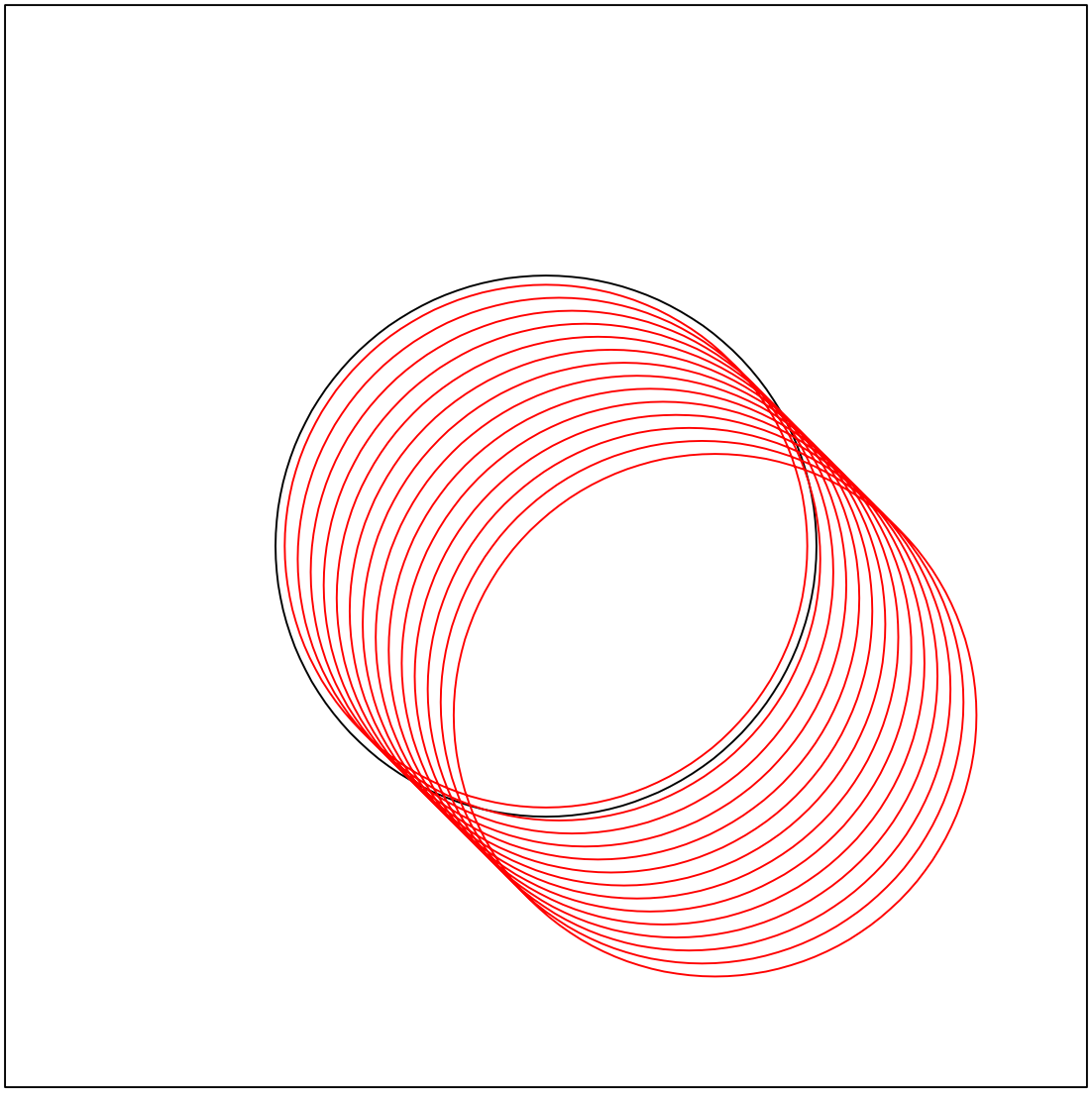

This is a layout of one lobe of the search path. The airplane would fly circles from one edge until nearly the middle. Then would start at the other edge of the circle and work back the other way to cover the entire search area. Then turn who pattern 90 degrees and do it again to do redundant coverage. (483 ft diameter search circle flown by plane). This set assumes that there is +/- 10 meter error in GPS location and thus we will need to allow for overlap of that distance. Thus only 17 foot field of view per flight pass.

All cases assume minimum height ever flown in 100 ft and camera has a 45 degree field of view and is mounted so it points directly at the ground during a bank.

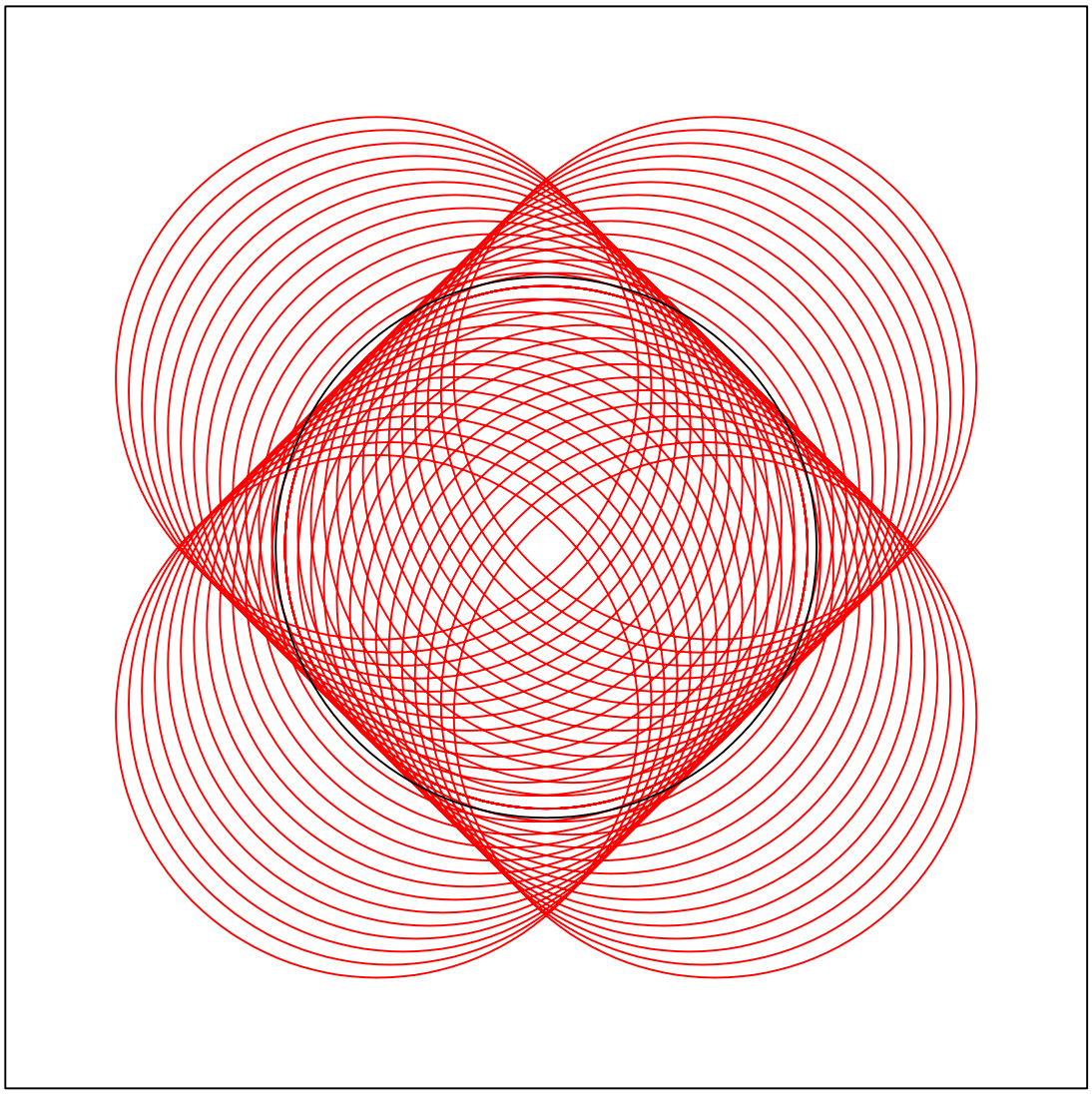

This is a layout of one lobe of the search path. The airplane would fly circles from one edge until nearly the middle. Then would start at the other edge of the circle and work back the other way to cover the entire search area. Then turn who pattern 90 degrees and do it again to do redundant coverage. (483 ft diameter search circle flown by plane). This set assumes that there is +/- 10 meter error in GPS location and thus we will need to allow for overlap of that distance. Thus only 17 foot field of view per flight pass.

APPENDIX B: ACTUAL FLIGHT PATH DESIGN

This set assumes that there is +/- 10 meter error in GPS location and thus we will need to allow for overlap of that distance. Thus only 17 foot field of view per flight pass.

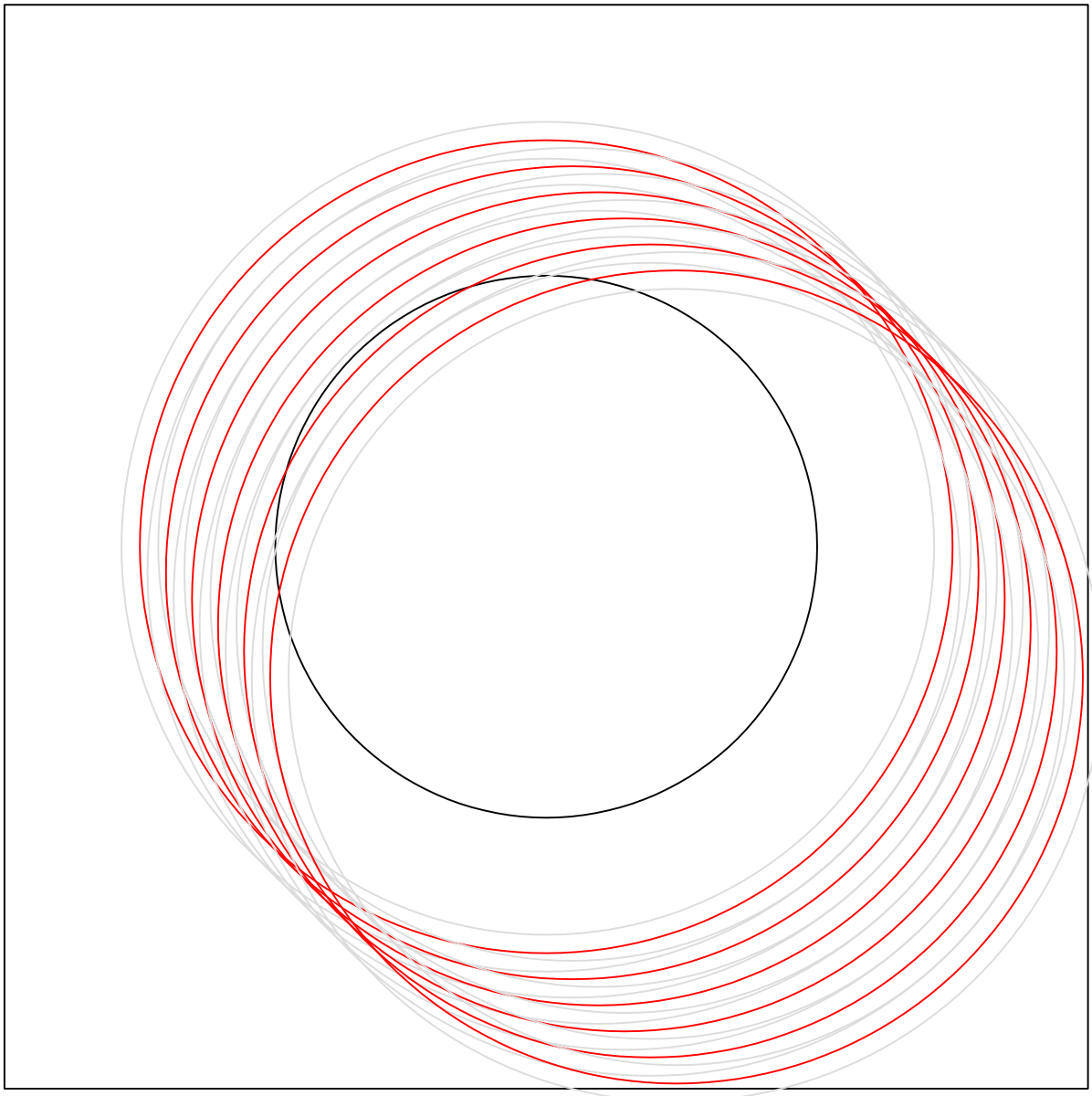

750 ft circles will not work. We don't cover much of the target area before we are well out of the fly zone into the no fly zones. This assumes +/- 10 m error in GPS location which is probably reasonable. Even without error 750 ft will not work.